Inorg. Chem. **2003**, *42*, 5399–5404

Long-Range Ferromagnetic Ordering in Two-Dimensional Coordination Polymers $Co[N(CN)_2]_2(L)$ [L = Pyrazine Dioxide (pzdo) and 2-Methyl Pyrazine Dioxide (mpdo)] with Dual μ- and μ_3-$[N(CN)_2]$ Bridges

Hao-Ling Sun,[†] Song Gao,*[,†] Bao-Qing Ma,[†] and Gang Su[‡]

College of Chemistry and Molecular Engineering, State Key Laboratory of Rare Earth Materials Chemistry and Applications, PKU-HKU Joint Laboratory on Rare Earth Materials and Bioinorganic Chemistry, Peking University, Beijing 100871, China, and Department of Physics, The Graduate School of the Chinese Academy of Sciences, P.O. Box 3908, Beijing 100039, China

Received February 23, 2003

Two novel coordination polymers of Co(II) with dicyanamide (dca) were obtained by the addition of ancillary ligands of pyrazine dioxide (pzdo) and 2-methyl pyrazine dioxide (mpdo) into the Co–dca binary system, respectively. $Co[N(CN)_2]_2$(pzdo) (**1**) crystallizes in the orthorhombic space group of *Pnnm* (No. 58) with $a = 9.4699(5)$ Å, $b = 14.9984(3)$ Å, $c = 7.4313(7)$ Å, and $Z = 4$, while $Co[N(CN)_2]_2$(mpdo) (**2**) is in the monoclinic space group *C*2 (No. 5) with $a = 16.5391(4)$ Å, $b = 9.6065(2)$ Å, $c = 7.5001(2)$ Å, $\beta = 105.779(1)°$, and $Z = 4$. Both complexes contain similar two-dimensional triangular Co–dca layers, which offer rare examples of mixed 1,5-μ- and μ_3-dca bridging coordination polymers with long-range ferromagnetic ordering below ca. 2.5 K.

The design and synthesis of metal coordination polymers are currently under intense investigation in the context of molecule-based magnets. One common approach is employed to connect paramagnetic transition metal ions via bridging ligands into multidimensional networks, in which the metal ions are the source of magnetic moments, while the bridging ligands provide the superexchange pathways between the magnetic centers. A variety of magnetic coordination polymers bridged by small conjugated ligands, such as cyano, oxalato, and azido, have been reported in the last two decades, and these were shown to have good superexchange properties.[1−3] The dca (dicyanamide) ligand, $[N(CN)_2]^-$, possesses three coordination nitrogen atoms and several possible coordination modes: terminal, bidentate 1,5-μ-, three-coordinate μ_3-, and unusual μ_4-dca, thus providing a versatile "building block" for constructing multidimensional networks. Series of rutile-like complexes $M[N(CN)_2]_2$ (M = Cr, Mn, Fe, Co, Ni, Cu) have been shown to be magnetically ordering (except M = Cu); namely, they are weak ferromagnets for M = Cr, Mn, and Fe below 47, 16, and 19 K, respectively, and ferromagnets for M = Co and Ni below 9 and 21 K, respectively.[4] The magnetic order results essentially from the three-atom pathway of the μ_3-dca.

Although the addition of ancillary ligands (e.g., pyridine, pyrazine, pyrimidine, 2,2′-bipyrimidine, 4,4′-bipyridine, and 2,2′-bipyridine, etc.) into these binary systems frequently

* To whom correspondence should be addressed. E-mail: gaosong@pku.edu.cn. Phone: 0086-10-62756320. Fax: 0086-10-62751708.
[†] Peking University.
[‡] The Graduate School of the Chinese Academy of Sciences.

(1) (a) Dunbar, K. R.; Heintz, R. A. *Prog. Inorg. Chem.* **1997**, *54*, 118 and references therein. (b) Ferlay, S.; Mallah, T.; Ouahes, R.; Veillet, P.; Verdaguer, M. *Nature* **1995**, *378*, 701. (c) Sato, O.; Iyoda, T.; Fujishima, A.; Hashimoto, K. *Science* **1996**, *272*, 704. (d) Larionova, J.; Sanchiz, J.; Gohlen, S.; Ouahab, L.; Kahn, O. *Chem. Commun.* **1998**, 953. (e) Holmes, S. M.; Girolami, G. S. *J. Am. Chem. Soc.* **1999**, *121*, 5593. (f) Hatlevik, O.; Buschmann, W. E.; Zhang, J.; Manson, J. L.; Miller, J. S. *Adv. Mater.* **1999**, *11*, 914. (g) Kou, H. Z.; Gao, S.; Sun, B. W.; Zhang, J. *Chem. Mater.* **2001**, *13*, 1431. (h) Ma, B. Q.; Gao, S.; Su, G.; Xu, G. X. *Angew. Chem., Int. Ed.* **2001**, *40*, 734. (i) Yeung, W. F.; Man, W. L.; Wong, W. T.; Lau, T. C.; Gao, S. *Angew. Chem., Int. Ed.* **2001**, *40*, 3031.

(2) For example: (a) Tamaki, H.; Zhong, Z. J.; Matsumoto, N.; Kida, S.; Koikawa, K.; Achiwa, N.; Okawa, H. *J. Am. Chem. Soc.* **1992**, *114*, 6974. (b) Mathoniere, C.; Nuttall, C. J.; Carling, S. G.; Day, P. *Inorg. Chem.* **1996**, *35*, 1201. (c) Decurtins, S.; Schmalle, H. W.; Schneuwly, P.; Ensling, J.; Gütlich, P. *J. Am. Chem. Soc.* **1994**, *116*, 9521.

(3) For example: (a) Ribas, J.; Escuer, A.; Monfort, M.; Vicente, R.; Cortes, R.; Lezama, L.; Rojo, T. *Coord. Chem. Rev.* **1999**, *193*−*195*, 1027 and references therein. (b) Monfort, M.; Resino, I.; Ribas, J.; Stoeckli-Evans, H. *Angew. Chem., Int. Ed.* **2000**, *39*, 191. (c) Hong, C. S.; Do, Y. *Angew. Chem., Int. Ed.* **1999**, *38*, 193. (d) Manson, J. L.; Arif, A. M.; Miller, J. S. *Chem. Commun.* **1999**, 1479. (e) Shen, H. Y.; Bu, W. M.; Gao, E. Q.; Liao, D. Z.; Jiang, Z. H.; Yan, S. P.; Wang, G. L. *Inorg. Chem.* **2000**, *39*, 396. (f) Thompson, L. K.; Tandon, S. S.; Lloret, F.; Cano, J.; Julve, M. *Inorg. Chem.* **1997,** *36*, 3301. (g) Ma, B. Q.; Sun, H. L.; Gao, S.; Su, G. *Chem. Mater.* **2001**, *13*, 1946. (h) Shen, Z.; Zuo, J. L.; Gao, S.; Song, Y.; Che, C. M.; Fun, H. K.; You, X. Z. *Angew. Chem., Int. Ed.* **2000**, *39*, 3633.

10.1021/ic034202i CCC: $25.00
Published on Web 07/25/2003

alters the bridging mode of $[N(CN)_2]^-$ from μ_3 to 1,5-μ, and therefore leads to a paramagnetic behavior,[4f,6] a wide variety of molecular architectures subsequently obtained conduce to establish a better understanding of the relationship between structure and magnetic behavior.[5,6] To date, only a few dca complexes containing ancillary ligands show long-range ordering behavior[5] which is directly related to either the spatial dimensionality of the crystal structures[5a−c] or the coexistence of the μ_3- and 1,5-μ-dca pathways.[5d−f] Here, we report two novel two-dimensional (2D) complexes Co-$[N(CN)_2]_2$(pzdo) (pzdo = pyrazine dioxide) (**1**) and Co-$[N(CN)_2]_2$(mpdo) (mpdo = 2-methyl pyrazine dioxide) (**2**) consisting of both μ_3- and 1,5-μ-bridging modes of dca with long-range ferromagnetic ordering.

Experimental Section

Elemental analyses of carbon, hydrogen, and nitrogen were carried out with an Elementar Vario EL. The variable-temperature dc magnetic susceptibility, the zero-field ac magnetic susceptibility, and the field dependence of magnetization were performed on a Maglab System 2000 magnetometer (Oxford Instruments).[7] The experimental susceptibilities were corrected for the diamagnetism of the constituent atoms (Pascal's tables).[8]

Synthesis. Pyrazine dioxide (pzdo) and 2-methyl pyrazine dioxide (mpdo) were prepared from pyrazine and 2-methylpyrazine by means of a known method.[9] Sodium dicyanoamide (Na(dca)) and other chemicals were purchased, and these were used directly without further purification.

Co[N(CN)$_2$]$_2$(pzdo), 1. $CoCl_2 \cdot 6H_2O$ (0.25 mmol) and 0.50 mmol of Na(dca) were dissolved in 10 mL of water. Aqueous solution (10 mL) of pzdo (0.50 mmol) was added with continuous stirring. The resulting solution was filtrated and allowed to slowly evaporate at room temperature. After one month, deep-red single crystals suitable for X-ray diffraction appeared. The crystals were collected, washed with water, and dried in air (yield 60%). Anal. Calcd for $C_8H_4CoN_8O_2$: C, 31.69, H, 1.33; N, 36.97%. Found: C, 31.60, H, 1.49, N, 36.66%. IR (cm^{-1}, KBr disk): 2318 ms, 2293 ms, 2269 ms, 2247m, 2211 s, 2180 s. The polycrystalline sample of **1** with higher purity was prepared by fast precipitation from the concentrated aqueous solution of $CoCl_2 \cdot 6H_2O$, pzdo, and dca with a ratio of 1:1:2. The powder sample of 3D α-Co(dca)$_2$ (**1a**) was prepared through the same method from the concentrated solution of $CoCl_2 \cdot 6H_2O$ and dca with a ratio of 1:2.

Co[N(CN)$_2$]$_2$(mpdo), 2. A method similar to that for compound **1** with mpdo instead of pzdo was used to prepare compound **2**. Large deep-red single crystals and very tiny pink crystals were obtained. The deep-red crystals were identified as **2**, while pink crystals were also regarded as **2** but contaminated by Co(dca)$_2$. The former crystals were separated out mechanically (yield 50%), and these crystals were used for structural and magnetic investigation. Anal. Calcd for $C_9H_6CoN_8O_2$: C, 34.09; H, 1.91; N, 35.33%. Found: C, 33.06; H, 1.92; N, 35.46%. IR (cm^{-1}, KBr disk): 2316 ms, 2290 ms, 2274 ms, 2246 m, 2207 s, 2172 s.

Crystallography. A deep-red crystal of **1** (0.25 × 0.15 × 0.10 mm^3) and a crystal of **2** (0.15 × 0.15 × 0.15 mm^3) were selected for the single crystal X-ray diffraction analysis. All the data collections were carried out on a Nonius Kappa CCD diffractometer with graphite-monochromated Mo Kα radiation (λ = 0.71073 Å) at 293 K. The structures were solved by direct methods and refined by a full-matrix least-squares technique based on F^2 using the SHELXL 97 program. All non-hydrogen atoms were refined anisotropically, and hydrogen atoms were placed on the calculated positions and were refined isotropically. The details of the crystal data and selected bond lengths and angles for compounds **1** and **2** are listed in Tables 1 and 2, respectively.

Table 1. Crystal Data and Structure Refinement for **1** and **2**

	1	**2**
formula	$C_8H_4CoN_8O_2$	$C_9H_6CoN_8O_2$
fw	303.12	317.15
cryst syst	orthorhombic	monoclinic
space group	*Pnnm* (No. 58)	*C*2 (No. 5)
a (Å)	9.4699(5)	16.5391(4)
b (Å)	14.9984(3)	9.6065(2)
c (Å)	7.4313(7)	7.5001(2)
α (deg)	90	90
β (deg)	90	105.779(1)
γ (deg)	90	90
V (Å^3)	1055.49(12)	1146.73(5)
Z	4	4
D_{calcd} (Mg/m^3)	1.908	1.837
μ (mm^{-1})	1.640	1.514
GOF	1.118	1.018
F(000)	604	636
R_{int}	0.0866	0.0346
R1[a] [$I > 2\sigma$(I)]	0.0392	0.0349
wR2[b] [$I > 2\sigma$ (I)]	0.0965	0.0891

[a] $R1 = \sum||F_o| - |F_c||/\sum|F_o|$. [b] $wR2 = [\sum w(F_o^2 - F_c^2)^2/\sum w(F_o^2)^2]^{1/2}$.

Results and Discussion

Description of Structures. The introduction of ancillary ligands, pzdo for **1** and mpdo for **2**, into the M(dca)$_2$ system

(4) (a) Batten, S. R.; Jensen, P.; Moubaraki, B.; Murray, K. S.; Rubson, R. *Chem. Commun.* **1998**, 439. (b) Manson, J. L.; Kmety, C. R.; Huang, Q. Z.; Lynn, J. W.; Bendele, G. M.; Pagola, S.; Stephens, P. W.; Liable-Sands, L. M.; Rheingold, A. L.; Epstein, A. J.; Miller, J. S. *Chem. Mater*. **1998**, *10*, 2552. (c) Kurmoo, M.; Kepert, C. J. *New J. Chem.* **1998**, 1515. (d) Kmety, C. R.; Huang, Q. Z.; Lynn, J. W.; Erwin, R. W.; Manson, J. L.; McCall, S.; Crow, J. E.; Stevenson, K. L.; Miller, J. S.; Epstein, A. J. *Phys. Rev. B* **2000**, *62*, 5576. (e) Manson, J. L.; Kmety, C. R.; Palacio, F.; Epstein, A. J.; Miller, J. S. *Chem. Mater*. **2001**, *13*, 1068. (f) Miller, J. S.; Manson, J. L. *Acc. Chem. Res.* **2001**, *34* (7), 563.

(5) (a) Manson, J. L.; Huang, Q. Z.; Lynn, J. W.; Koo, H. J.; Whangbo, M. H.; Bateman, R.; Otsuka, T.; Wada, N.; Argyriou, D. N.; Miller, J. S. *J. Am. Chem. Soc.* **2001**, *123*, 162. (b) Kusaka, T.; Ishida, T.; Hashizume, D.; Iwasaki, F.; Nogami, T.; *Chem. Lett.* **2000**, 1146. (c) Yeung, W. F.; Gao, S.; Wong, W. T.; Lau, T. C. *New J. Chem.* **2002**, 523. (d) Jensen, P.; Batten, S. R.; Moubaraki, B.; Murray, K. S. *Chem. Commun*. **2000**, 793. (e) Kutasi, A. M.; Batten, S. R.; Moubaraki, B.; Murray, K. S. *J. Chem. Soc., Dalton Trans.* **2002**, 819. (f) Jensen, P.; Price, D. J.; Batten, S. R.; Moubaraki, B.; Murray, K. S. *Chem. Eur. J.* **2000**, *6*, 3186.

(6) (a) Manson, J. L.; Schlueter, J. A.; Geiser, U.; Stone, M. B.; Reich, D. H.; *Polyhedron* **2001**, *20*, 1423. (b) Marshall, S. R.; Incarvito, C. D.; Manson, J. L.; Rheingold, A. L.; Miller, J. S. *Inorg. Chem.* **2000**, *39*, 1969. (c) Manson, J. L.; Afrif, A. M.; Incarvito, C. D.; Liable-Sands, L. M.; Rheingold, A. L.; Miller, J. S. *J. Solid State Chem.* **1999**, *145*, 369. (d) van der Werff, P. M.; Batten, S. R.; Jensen, P.; Moubaraki, B.; Murray, K. S. *Inorg. Chem*. **2001**, *40*, 1718. (e) Batten, S. R.; Jensen, P.; Kepert, C. J.; Kurmoo, M.; Moubaraki, B.; Murray, K. S.; Price, D. J. *J. Chem. Soc., Dalton Trans*. **1999**, 2987. (f) Dasna, L.; Golhen, S.; Ouahab, L.; Pena, O.; Guillevic, J.; Fettouhi, M. J. *J. Chem. Soc., Dalton Trans*. **2000**, 129. (g) Sun, B. W.; Gao, S.; Ma, B. Q.; Wang, Z. M. *New. J. Chem.* **2000**, 953. (h) Sun, B. W.; Gao, S.; Ma, B. Q.; Niu, D. Z.; Wang, Z. M. *J. Chem. Soc., Dalton Trans.* **2000**, 4187. (i) Sun, B. W.; Gao, S.; Ma, B. Q.; Wang, Z. M. *Inorg. Chem. Commun.* **2001**, *4*, 72.

(7) Oxford Instruments, MagLab 2000 system, a multifunctional physical property measurement system including dc/ac magnetic measurements, resistance, and heat capacity measurements, etc., in 1.8−400 K temperature range and ±7 T superconductor magnetic field.

(8) *Theory and Application of Molecular Paramagnetism*; Boudreaux, E. A., Mulay, J. N., Eds.; J. Wiley and Sons: New York, 1976.

(9) Simpon, P. G.; Vinciguerra, A.; Quagliano, J. V. *Inorg. Chem.* **1963**, *2*, 282.

Table 2. Selected Bond Lengths (Å) and Angles (deg) for **1** and **2**

		1[a]	
Co(1)−N(3)	2.100(3)	Co(1)−O(1)	2.138(4)
Co(2)−N(5)	2.089(3)	Co(2)−N(4)	2.179(4)
N(3)a−Co(1)−N(3)	86.90(16)	N(3)b−Co(1)−N(3)	93.10(16)
N(3)−Co(1)−O(1)c	90.22(12)	N(3)−Co(1)−O(1)	89.78(12)
O(1)c−Co(1)−O(1)	180.0		
N(5)−Co(2)−N(5)d	180.0	N(5)−Co(2)−N(5)e	93.80(19)
N(5)−Co(2)−N(5)f	86.20(19)	N(5)−Co(2)−N(4)d	90.88(13)
N(5)−Co(2)−N(4)	89.12(13)	N(4)d−Co(2)−N(4)	180.0
		2[b]	
Co(1)−O(1)	2.067(2)	Co(1)−N(3)	2.136(3)
Co(1)−N(6)b	2.156(4)	Co(2)−N(4)	2.181(5)
Co(2)−N(5)	2.203(5)	Co(2)−N(7)	2.102(3)
Co(2)−N(9)a	2.098(3)		
O(1)−Co(1)−O(1)a	176.8(2)	O(1)−Co(1)−N(3)	89.63(14)
O(1)−Co(1)−N(3)a	88.21(13)	N(3)−Co(1)−N(3)a	94.31(19)
O(1)−Co(1)−N(6)b	90.42(13)	N(3)−Co(1)−N(6)b	179.53(17)
O(1)−Co(1)−N(6)c	91.75(13)	N(3)−Co(1)−N(6)c	86.16(9)
N(6)b−Co(1)−N(6)c	93.37(19)	N(9)a−Co(2)−N(7)	85.91(11)
N(9)d−Co(2)−N(7)	94.08(11)	N(7)e−Co(2)−N(7)	179.7(3)
N(9)a−Co(2)−N(4)	90.16(14)	N(7)−Co(2)−N(4)	90.14(15)
N(9)a−Co(2)−N(5)	89.84(14)	N(7)−Co(2)−N(5)	89.86(15)
N(4)−Co(2)−N(5)	180.0	N(9)a−Co(2)−N(9)d	179.7(3)

[a] Symmetry code: a, $-x-1, -y, z$; b, $x, y, -z+1$; c, $-x-1, -y, -z+1$; d, $-x, -y, -z$; e, $x, y, -z$; f, $-x, -y, z$. [b] Symmetry code: a, $-x, y, -z$; b, $-x, y-1, -z$; c, $x, y-1, z$; d, $x, y, z+1$; e, $-x, y, -z+1$.

changes the structure from a three-dimensional rutile-like geometry to a 2D triangular motif, in accompanying the formation of dual μ_3- and 1,5-μ-modes in **1** and **2**. These structures thus offer rare examples of both bridging modes coexisting in one compound.

Compound 1. It is composed of two crystallographically independent cobalt atoms with different coordination environments, as shown in Figure 1. One may see that Co(1) is coordinated in an octahedron by four nitrile nitrogen atoms at equatorial sites with the Co−N distance of 2.099(3) Å and two oxygen atoms of pzdo at the axial sites with the Co−O distance of 2.124(4) Å. Each Co(1) is connected to four nearest Co(2) atoms through μ_3-dca with the Co(1)···Co(2) separation of 6.019 Å (Figure 1a). Both the Co−N distance and Co(1)···Co(2) separation are similar to those found in the 3D α-Co(dca)$_2$ (**1a**).[4] Each octahedral Co(2) is coordinated by four nitrile nitrogen atoms at the equatorial sites with the Co−N distance of 2.082(3) Å and two amide nitrogen atoms at the axial sites with the Co−N distance of 2.180 Å. Co(2) joins to the two nearest Co(2) ions through double 1,5-μ-dca bridges along the *a* axis with the Co(2)···Co(2) separation of 7.431 Å and four nearby Co(1) atoms through μ_3-dca (Figure 1b). Thus, Co(II) ions are connected by dual 1,5-μ- and μ_3-$[N(CN)_2]^-$ bridges, yielding a 2D triangular lattice in the *ac* plane by connecting metal ions (Figure 2). Terminal pzdo ligands[3g] form weak hydrogen bonds with other pzdo molecules from adjacent layers, extending the 2D sheets into a three-dimensional (3D) network with interlayer Co···Co separation being 7.499 Å (Fig. S1).

Compound 2. Using mpdo instead of pzdo gives a similar 2D layer, as found in **1**. All Co ions in **2** lie on a 2-fold axis, and the coordination environments are the same as those found in **1** (Figure 3). The same orientation of asymmetric

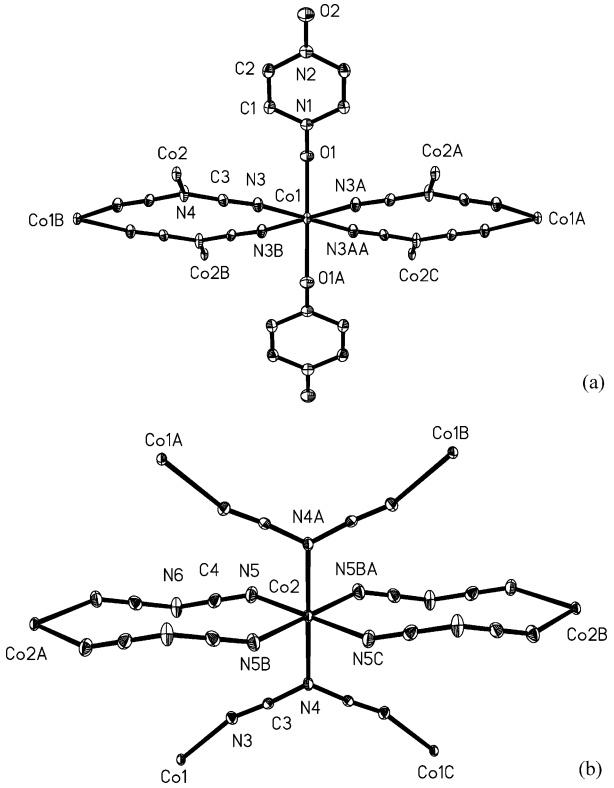

Figure 1. Coordination environment of Co(1) (a) and Co(2) (b) of compound **1**.

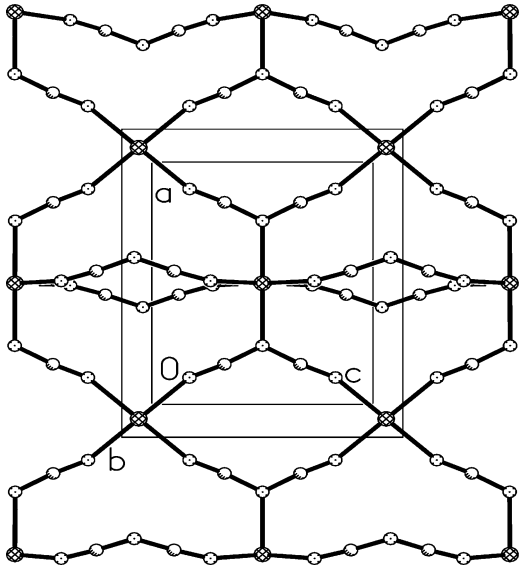

Figure 2. Two-dimensional *ac* plane in **1** formed by dual 1,5-μ- and μ_3-$[N(CN)_2]^-$ bridges.

terminal mpdo ligands along the *b* axis (Figures 3a and 4) generates the polarity of compound **2**. The dca anion also exhibits both μ_3- and 1,5-μ-coordination modes with the Co···Co distances of 6.078 and 7.500 Å, respectively. The Co···Co, Co−N, and Co−O distances are similar to those found in compound **1** and in the rutile-like 3D structures of M(dca)$_2$. The Co(II) ions connected by μ_3- and 1,5-μ-dca ligands form a triangular lattice in the *bc* plane. No pronounced hydrogen bonding interaction, except the van der Waals force, between the 2D layers takes effect. The interlayer Co···Co distance is 8.270 Å (Figure 4).

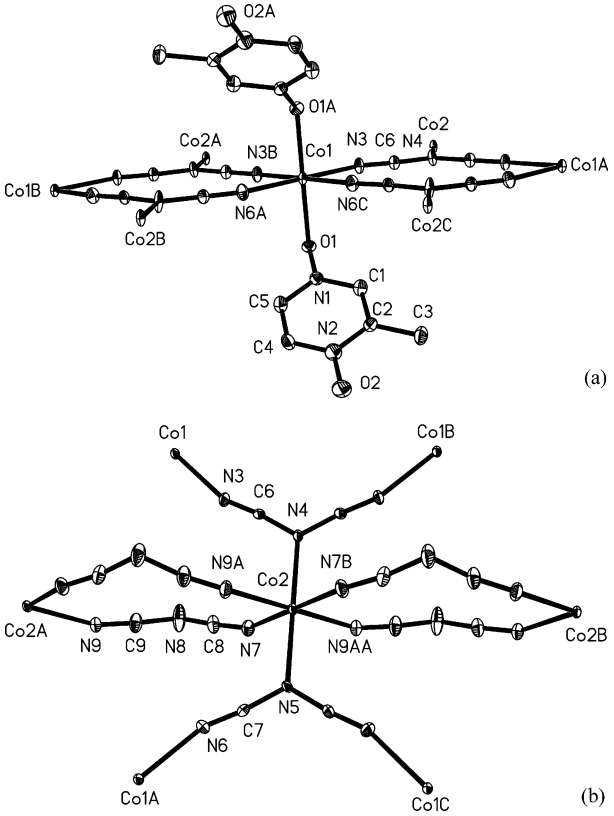

Figure 3. Coordination environment of Co(1) (a) and Co(2) (b) of compound **2**.

The 2D triangular structural motifs of **1** and **2** are similar to those found in $M(dca)_2(H_2O)(phz)$ (M = Co, or Ni and phz = phenazine),[5e] but the layers in the latter are well separated by bulky ligands (Co···Co = 11.194 Å). Nevertheless, the interlayer interaction of strong N···H−O hydrogen bonding in the latter is comparable with the weak hydrogen bonding of O···H−C or the van der Waals force in the title compounds.

Magnetic Properties. Compound 1. A powder sample of **1** was magnetically studied on an Oxford MagLab-2000 system. A plot of $\chi_M T$ versus T (per Co unit) in a field of 5 kOe is shown in Figure 5a. The $\chi_M T$ value at 300 K is 3.08 $cm^3\ mol^{-1}$ K, which decreases smoothly with a decrease of temperature and reaches a minimum value of 2.50 $cm^3\ mol^{-1}$ K at 19.3 K. On further cooling, $\chi_M T$ increases rapidly and reaches two maxima of 3.07 and 3.15 $cm^3\ mol^{-1}$ K at 7.9 and 2.2 K, respectively. The magnetic susceptibility above 40.0 K obeys the Curie−Weiss law with the Weiss constant, $\theta = -9.4$ K, and the Curie constant, $C = 3.17$ $cm^3\ mol^{-1}$ K. The C value corresponds to $g = 2.60$ and an effective magnetic moment of 5.03 μ_B per Co(II) ion, which is significantly larger than the spin-only value, being attributed to the orbital contribution of high spin Co(II) ions in the octahedral environment, but is consistent with the values observed in the 3D α-$Co(dca)_2$ (**1a**) complex[4b] and many other high spin octahedral Co(II) complexes.[8] The decrease of $\chi_M T$ at high temperature does not imply antiferromagnetic coupling between Co(II) ions, as it is mainly due to the single-ion behavior of Co(II). Its $^4T_2$ triplet ground state splits under the combination of a spin−orbit coupling and a noncubic crystal field, giving six Kramers doublets with an effective anisotropic $S = {}^1/_2$ ground state. The divergence of $\chi_M T$ below 20 K results from the ferromagnetic couplings between the effective spins of adjacent Co(II) ions.[10] The FCM and ZFCM curves measured in a low field of 100 Oe show two abrupt increases in M at ca. 8.5 and 2 K, indicating the occurrence of two long-range ferromagnetic transitions (inset of Figure 5a). The temperature dependence of ac magnetic susceptibility also verifies the magnetic phase transitions below ca. 9 and 3 K (T_c) defined by the point where nonzero χ'' appears. No frequency dependence was observed, thus excluding any glassy behavior (Figure 6a).

The field dependence of the magnetization measured at 1.75 K shows a rapid saturation of the magnetization. The saturated value of the magnetization is 2.28 $N\beta$ per Co at 70 kOe, which corresponds to a $g_{eff} = 4.56$ with $S_{eff} = {}^1/_2$ per Co(II) ion (Figure S3). The g value is slightly smaller than that for a 3D α-$Co(dca)_2$[4] and is comparable to those of other complexes with octahedral coordination of Co(II) ions. The rapid increase in the saturation at low temperature for **1** is quite typical for long-range ferromagnetic ordering. Hysteresis measured at 1.74 K reveals that it is a soft magnet.

Observation of two ferromagnetic transitions in such a 2D system is not easy to understand at first glance. To gain more insight, XRD patterns were experimentally recorded and theoretically calculated on the basis of the single crystal X-ray diffraction result, for the same sample used in the magnetic measurements. The results show that the sample is dominated by compound **1** but contaminated with trace 3D α-$Co(dca)_2$ (**1a**). The poor solubility of **1** in common solvents prevents its further purification. The fast precipitation method, though, can eliminate the impurity to some extent, but the sample is still not pure enough. Since the possible slight contamination of 3D α-$Co(dca)_2$, we may reasonably assume that the observation of the transition at 8−9 K could be regarded as a result of trace 3D α-$Co(dca)_2$ (**1a**), while the low-temperature ferromagnetic transition at ca. 2 K should be the intrinsic property from complex **1**. To elucidate this assumption unambiguously, the ZFCM, FCM, and ac susceptibility were measured for the sample mixing 10% 3D α-$Co(dca)_2$ (**1a**) with **1**. As shown in Figure 5a,c, above 9 K there is no difference of the ZFCM and FCM susceptibility for both **1** and the mixed sample; however, in a temperature range 2−9 K, the signal of FCM for the mixed sample is remarkably stronger than that of **1**, indicating that the ordering around 9 K is caused by the impurity of 3D α-$Co(dca)_2$. At about 2 K, the signals of ZFCM and FCM for both **1** and the mixed sample increase sharply (Figure 5a,c), while no such a transition is observed for 3D α-$Co(dca)_2$ (**1a**) around 2 K (Figure 5b), suggesting that the magnetic ordering below 2 K is caused by **1**. The obviously stronger in-phase and out-of-phase signals on the ac curves for the mixed sample at about 9 K versus the disappearance of the transition for 3D α-$Co(dca)_2$ at 2 K with respect to dual signals of **1** demonstrates once again that the transitions

(10) Angelov, S.; Drillon, M.; Zhecheva, E.; Stoyanova, R.; Belaiche, M.; Derory, A.; Herr, A. *Inorg. Chem.* **1992**, *31*, 1514.

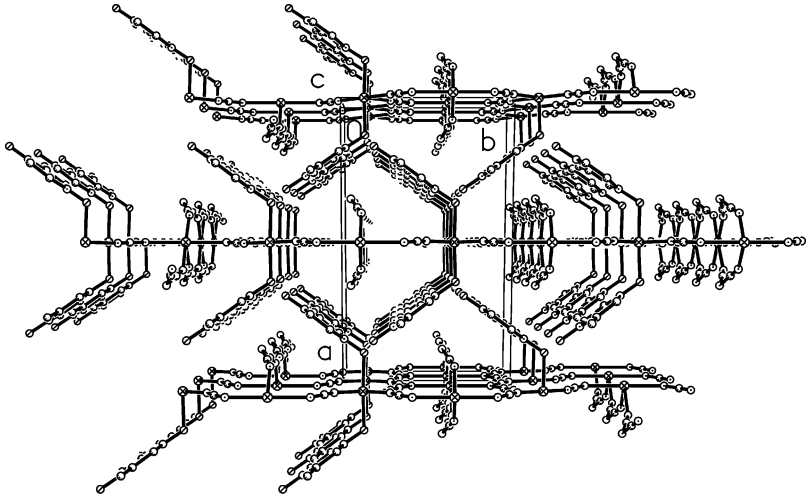

Figure 4. Stacking of 2D trigonal layer of **2**.

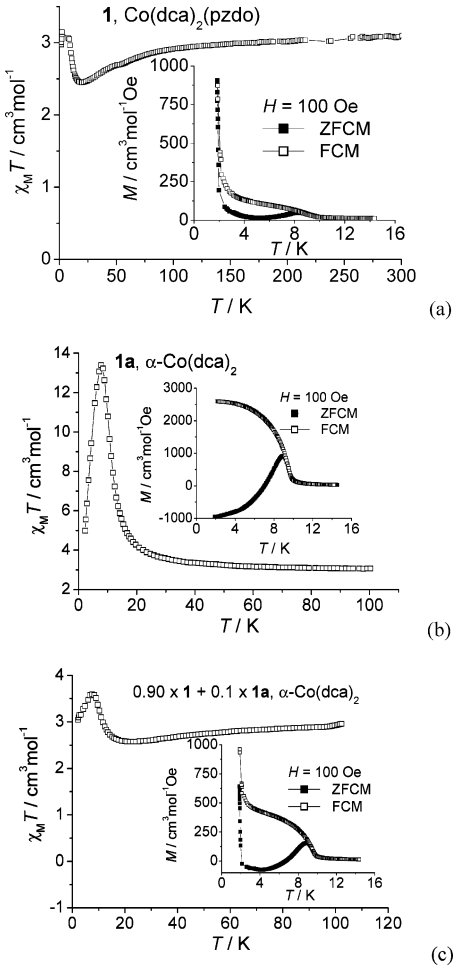

Figure 5. Temperature dependence of $\chi_M T$ for **1** (a), α-Co(dca)$_2$ (b), and $0.9 \times$ **1** $+ 0.1 \times$ **1a**, α-Co(dca)$_2$ (c). Inset: Zero field cooled magnetization (ZFCM) and field cooled magnetization (FCM) versus T measured at 100 Oe.

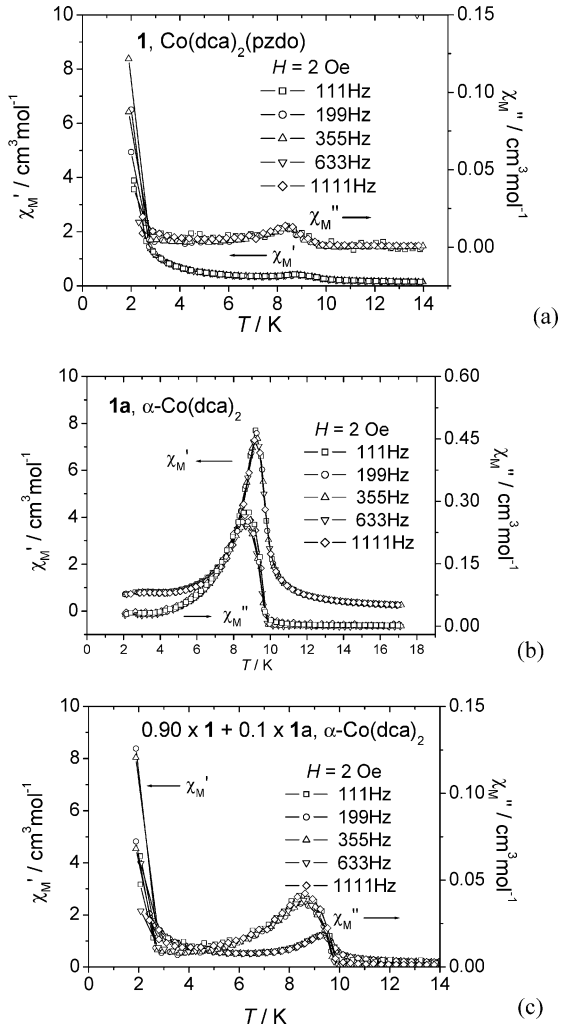

Figure 6. In-phase (χ_m') and out-phase (χ_m'') ac magnetic susceptibilities as a function of temperature taken at 111, 199, 355, 633, and 1111 Hz for **1** (a), α-Co(dca)$_2$ (b), and $0.9 \times$ **1** $+ 0.1 \times$ **1a**, α-Co(dca)$_2$ (c).

around 9 and 2 K are caused by 3D α-Co(dca)$_2$ and **1**, respectively (Figure 6).

Compound 2. The magnetic behavior of **2** should resemble that of **1** essentially on the basis of their similar layer structures. With the decrease of temperature, $\chi_M T$ goes down slowly to a minimum value of 2.60 cm^3 mol^{-1} K at 18.2 K and then goes up quickly to a maximum value of 3.06 cm^3 mol^{-1} K at 4.75 K (Figure 7). Fitting of the magnetic data above 50 K by the Curie−Weiss law gives the Weiss constant, $\theta = -13.7$ K, and the Curie constant, $C = 3.34$ cm^3 mol^{-1} K. The ZFCM and FCM data measured under

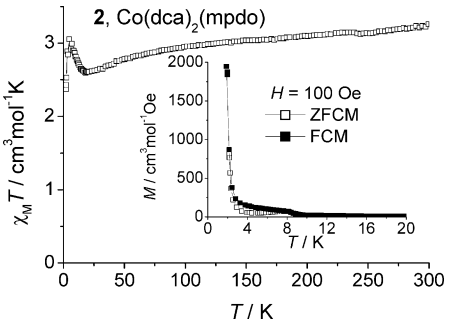

Figure 7. Temperature dependence of $\chi_M T$ for **2** measured at 5 kOe. Inset: Zero field cooled magnetization (ZFCM) and field cooled magnetization (FCM) versus T for **2** measured at 100 Oe.

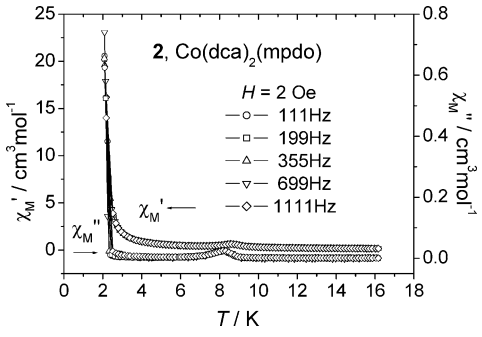

Figure 8. In-phase (χ_m') and out-of-phase (χ_m'') ac magnetic susceptibilities as a function of temperature taken at 111, 199, 355, 633, and 1111 Hz for **2**.

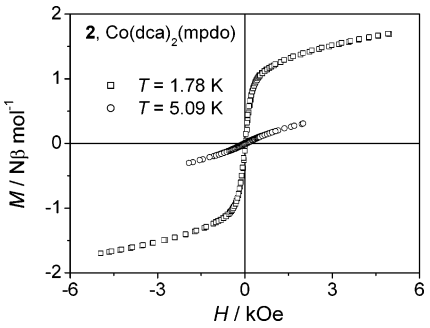

Figure 9. Magnetic hysteresis loops at 1.78 and 5.09 K for **2**.

the magnetic field of 100 Oe show an abrupt increase at 1.9 K and a small shoulder at 8.6 K, implying that the phase transitions take place for compound **2** (inset of Figure 7) and the trace 3D α-Co(dca)$_2$, respectively. The ac magnetic susceptibility also shows nonzero values of both in-phase and out-of-phase signals at about 8.2 and 2.5 K. The weaker shoulder at 8.2 K gives another evidence of the trace of 3D α-Co(dca)$_2$, while the sharp increase at 2.5 K suggests the occurrence of magnetic ordering for **2** (Figure 8). The hysteresis loop measured at 1.78 K reveals the behavior of a soft magnet of compound **2** (Figure 9).

In contrast to paramagnetic character above 2 K (though there might be magnetic order at much lower temperature) in 2D compound Co(dca)$_2$(H$_2$O)(phz),[5e] the FCM, ZFCM, and ac susceptibility for compounds **1** and **2** all present evidence of magnetic orderings below ca. 2.5 K. This would be related to the difference of interlayer Co···Co separation; namely, the separation is 7.499 Å for **1**, and 8.270 Å for **2**, which are significantly shorter than that in Co(dca)$_2$(H$_2$O)(phz) (11.194 Å). On the other hand, ordering temperatures T_c in **1** and **2** are comparable with that of a 3D network Co[N(CN)$_2$]$_2$ (pyrimidine) (1.8 K).[5b] However, they are considerably lower than that of 3D α-Co(dca)$_2$ (8−9 K), notwithstanding the same number of nearest neighbors, say 8, around each Co(2) ion. It is reasonable that the magnitude of Co···Co coupling in **1** and **2** should be smaller than that in 3D α-Co(dca)$_2$, since the Co···Co separations through μ- and μ_3-dca and interlayer separations (6.11 × 4, 7.45 × 2, and 7.499 × 2 Å for **1**, 6.078 × 4, 7.500 × 2, and 8.270 × 2 Å for **2**) are overall larger than those in the 3D α-Co(dca)$_2$ (6.00 × 2, 6.01 × 2, 7.07 × 2, 7.39 × 2 Å).

In summary, two novel title compounds are synthesized, which present rare examples of mixed $\mu_{1,5}$- and μ_3-dca bridging coordination polymers and have unusual 2D triangular lattice structures with long-range ferromagnetic ordering below 2.5 K.

Acknowledgment. This work was supported by the National Science Fund for Distinguished Young Scholars (20125104), the State Key Project of Fundamental Research (G1998061305), the Research Fund for the Doctoral Program of Higher Education (20010001020), and the Excellent Young Teachers Fund of MOE, P. R. China. We would like to thank Prof. Jian-Hua Lin for fitting XRD data and helpful discussions.

Supporting Information Available: Figure of the 3D network of **1** (Figure S1), comparison of the powder XRD spectra of **1** (Figure S2), and field dependence of magnetization and magnetic hystersis loops for **1**, α-Co(dca)$_2$ (**1a**), and a mixture of **1** and **1a** (0.9 × **1** + 0.1 × **1**a) (Figures S3 and S4). X-ray crystallographic file for **1** and **2**, in CIF format. This material is available free of charge via the Internet at http://pubs.acs.org.

IC034202I